nature communications

Article

https://doi.org/10.1038/s41467-022-35554-1

Importance of interface open circuit potential on aqueous hydrogenolytic reduction of benzyl alcohol over Pd/C

Received: 2 September 2022

Accepted: 9 December 2022

Published online: 27 December 2022

Check for updates

Guanhua Cheng[1,2], Wei Zhang[1,3], Andreas Jentys[1], Erika E. Ember[1], Oliver Y. Gutiérrez[4], Yue Liu[1,3] ✉ & Johannes A. Lercher[1,4] ✉

The open circuit potential (OCP) established by the quasi-equilibrated electrode reaction of H_2 and $H_3O^+_{(hydr.)}$, complicates catalytic reactions significantly. The hydrogenolysis rate of benzylic alcohol on Pd/C increases 2-3 orders of magnitude with the pH decreasing from 7 to 0.6. The reaction follows a pathway of protonated benzyl alcohol dehydration to a benzylic carbenium ion, followed by a hydride addition to form toluene. The dehydration of protonated benzyl alcohol is kinetic relevent, thus, being enhanced at lower pH. The OCP stabilizes all cationic species in the elementary steps. Particularly, the initial state (benzyl alcohol oxonium ion) is less stabilized than the dehydration transition state and the product (benzylic carbenium), thus, lowering the free energy barrier of the rate-determining step. In accordance, the rate increased with increasingly negative OCP. Beside OCP, an external negative electric potential in an electrocatlaytic system was also demonstrated to enhance the rate in the same way.

Catalyzed hydrogen additions such as hydrogenation and hydrogenolysis, are fundamental transformation for the synthesis of chemicals and energy carriers, typically catalyzed by transition metals[1–3]. The catalytic activity critically depends on the interactions between the reactive substrates and the active catalyst surface as well as on interactions with solvents and other reactive substrates. These interactions (de)stabilize ground and transition states, and therefore, influence the standard free energy barriers that determine reaction rates[4–6].

While such hydrogen addition reactions have been extensively studied and well understood at gas-solid interfaces[7,8], the presence of water induces additional complexity, as the electrochemical reactions at the interface lead to the generation of hydronium ions that may induce proton-coupled electron transfer (PCET)[9–11]. In addition, an open circuit potential (OCP) establishes spontaneously on the metal catalyst by the quasi-equilibrated electrode reaction of H_2 and $H_3O^+_{(hydr.)}$, establishing an electrostatic potential gradient from the metal surface to the bulk solution. It influences the excess chemical potentials of charged and neutral species and leads to a unique self-organization of the constituents at the metal-solvent interface[12]. Thus, not only the chemisorbed species on the metal, but also the (hydrated) ions and molecules at the outer Helmholtz plane, such as $H_3O^+_{(hydr.)}$, play an important role on determining the catalytic activity.

It has been reported previously that hydronium ions greatly enhance reaction rates catalyzed by Pt and Pt-group metals, by enabling an energetically favored PCET pathway[13–15] and by weakening the hydrogen binding standard free energy[16]. This points to the more general impact of the proton activity at the electrode surface plays on the thermodynamic state of the reacting substrates and, hence, on the catalytic pathways[17,18].

On a first view, the reductive one-step conversion of the alcohol C–O bond to a C-H bond and water resembles the hydrogenolytic

[1]Technische Universität München, Department of Chemistry and Catalysis Research Center, Lichtenbergstraβe 4, Garching D-85748, Germany. [2]Key Laboratory for Liquid-Solid Structural Evolution and Processing of Materials (Ministry of Education), School of Materials Science and Engineering, Shandong University, Jingshi Road 17923, Jinan 250061, PR China. [3]Shanghai Key Laboratory of Green Chemistry and Chemical Processes, School of Chemistry and Molecular Engineering, East China Normal University, Shanghai, PR China. [4]Institute for Integrated Catalysis, Pacific Northwest National Laboratory, 902 Battelle Boulevard, Richland, WA 99352, USA. ✉e-mail: liuyue@chem.ecnu.edu.cn; johannes.lercher@ch.tum.de

cleavage of C-C bonds. It has been reported that the activity and selectivity for this C–O bond cleavage is sensitive to the acidity of the catalyst support or the acidity of solvents[19–24], and that neutralizing the acid sites will eliminate the enhancement[22,25]. Extensive mechanistic studies for benzylic alcohol hydrogenolysis, led to the formulation of two main reaction mechanisms proposed, i.e., one hypothesizing that the C–O bond scission proceeds via a "bifunctional" dehydration-hydrogenation route[19,26], and another via a direct C-OH bond cleavage by hydrogen insertion[19,22,27,28]. Thus, the acid functionality either catalyzes dehydration or converts the carbonyl to a better leaving group. However, the elementary steps (which determine the catalytic pathway) involving $H_3O^+_{(hydr.)}$ and the metal in this conversion and in particular the role of the ionic environment at the interface are not understood and prevent formulating a generally accepted reaction mechanism.

Therefore, we address in this contribution the role of the OCP and hydronium ions at the metal surface and outer Helmholtz plane for benzyl alcohol hydrogenolysis on Pd/C in an aqueous environment. Pd has been chosen because of its high activity and selectivity towards C–O bond cleavage[29]. The pathway identified shows that the reaction proceeds via the protonation of the OH group making it a better leaving group (H_2O), leading to the formation of a benzylic carbocation, and yielding toluene after hydride addition (in contrast to the proton elimination in conventional dehydration). Using kinetic analysis and demonstrating kinetic isotope effects (KIE), we show that the dehydration of the protonated alcohol is the rate-determining step. The hydronium ions affect the reaction by changing the electric potential on Pd as well as the transition state concentration.

Results and discussion

Impact of the hydronium ion activity on benzyl alcohol hydrogenolysis

$$C_6H_5CH_2OH \xrightarrow{H_2/H_3O^+,Pd} C_6H_5CH_3 + H_2O \qquad \text{(Rxn1)}$$

Reductive elimination of water from benzyl alcohol on Pd/C involves cleavage of the C–O bond of benzyl alcohol to form toluene and water (Rxn 1). Products of aromatic ring hydrogenation, such as cyclohexylmethanol and methylcyclohexane, were not observed. The turnover frequency (TOF) decreased with increasing pH (Fig. 1a) and was very low above pH of 5, independently of the type of buffer solution used. This decrease suggests a critical role of hydronium ions for the catalytic conversion. In the absence of Pd, benzyl alcohol was not converted in acidic media (pH 1), demonstrating that the reaction is metal catalyzed. The reaction order in hydronium ions varies with the pH range from 0.6 to 7 (Fig. 1b).

Considering that hydronium ions are involved in the reaction, let us hypothesize that the elementary steps occur in the space ranging from the Pd surface itself to the outer Helmholtz plane. In this case the rate equation for the reaction (r_{BA}, subscript BA denoting benzyl alcohol) is:

$$r_{BA} = -\frac{dC_{BA}}{dt} = k_{eff} C_{BA}^{\alpha} P_{H_2}^{\beta} a_{H^+}^{\gamma} \qquad (1)$$

k_{eff} is the effective rate constant; a_{H^+} is the hydronium ion activity in the bulk phase, α, β and γ are the apparent reaction orders with respect to benzaldehyde, H_2 and $H_3O^+_{(hydr.)}$.

The reaction orders for both benzyl alcohol and H_2 were measured at pH 2.5 and pH 5 (Fig. S1 and Table 1). At pH 2.5, the reaction order in benzyl alcohol is slightly positive ($\alpha = 0.08$, Fig. S1a) and near 0^{th} order with respect to H_2 ($\beta = 0.09$, Fig. S1b). At pH 5, the reaction order with respect to both benzyl alcohol and H_2 are near 0 (Figs. S1c and S1d). The reaction order being 0^{th} or close to 0^{th} for organic substrate is common in hydrogenation and hydrogenolysis reactions[28,30–32], typically interpreted as a result of the high coverage of substrate. The reaction order of 0^{th} for H_2 indicates that either H coverage on Pd surface is also very high, i.e., near saturated coverage under noncompetitive adsorption with organic substrates or the adsorption sites are half occupied by both the substrates and H under competitive adsorption, or that the adsorbed H does not participate in the rate determining step.

In order to estimate whether the Pd surface has a substantial coverage of H, cyclic voltammetry on Pd/C (20 mg, 30 wt.%) with different concentrations of benzyl alcohol was measured at pH 2.5 (Fig. 2a) and pH 5 (Fig. 2b). In presence of benzyl alcohol, the peak of underpotentially deposited hydrogen was reduced (H_{upd}, 0.06–0.34 V vs. RHE at pH 2.5 and 0.09–0.43 V vs. RHE at pH 5), and totally disappeared at a concentration of 500 μM (Fig. 2a, b). Comparing the H_{upd} current in presence and absence of benzyl alcohol allows to determine the fraction of H that was inhibited (blocked) by benzyl alcohol (Fig. 2c, d). The drastically decreasing H_{upd} with increasing benzyl alcohol concentration indicates that benzyl alcohol binds much stronger than H on Pd, which will lead to a full coverage of the Pd surface by benzyl alcohol and a very low coverage with H under our reaction condition (benzyl alcohol concentration between 6 and 80 mM). Therefore, the possibility of a high coverage of H is excluded, and the observed near zero reaction order of H_2 in benzyl alcohol reaction indicates that the H adatoms are only involved in elementary steps after the rate determining step.

If this is the case, benzyl alcohol conversion should only have a small kinetic isotope effect for gaseous H_2 vs. D_2 (as shown indeed in Fig. 3). The conversion rate of benzyl alcohol has only small differences for reactions with H_2 and D_2 in either H_2O (rate ratio of 1.1) or D_2O (rate ratio of 1.0) at 298 K and 1 bar H_2 or D_2. In comparison, the ratio of the rate in H_2O to that in D_2O is 1.4 in H_2 and 1.3 in D_2. This sensitivity indicates that H or D from water or $H_3O^+_{(hydr.)}$ are involved in the kinetically relevant steps.

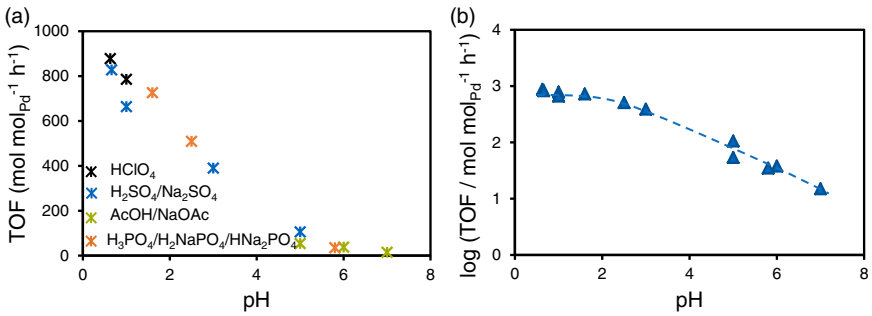

Fig. 1 | Influence of pH on the activity of benzyl alcohol hydrogenolysis. a TOF as a function of pH in the catalytic conversion of benzyl alcohol to toluene on Pd/C. **b** Log TOF as a function of pH to obtain the apparent reaction order in bulk hydronium ion with a dashed line as a guide to the eye. Reaction condition: 0.2 M buffer solution, 298 K and 1 bar H_2. The legend indicates different buffer compositions.

https://doi.org/10.1038/s41467-022-35554-1

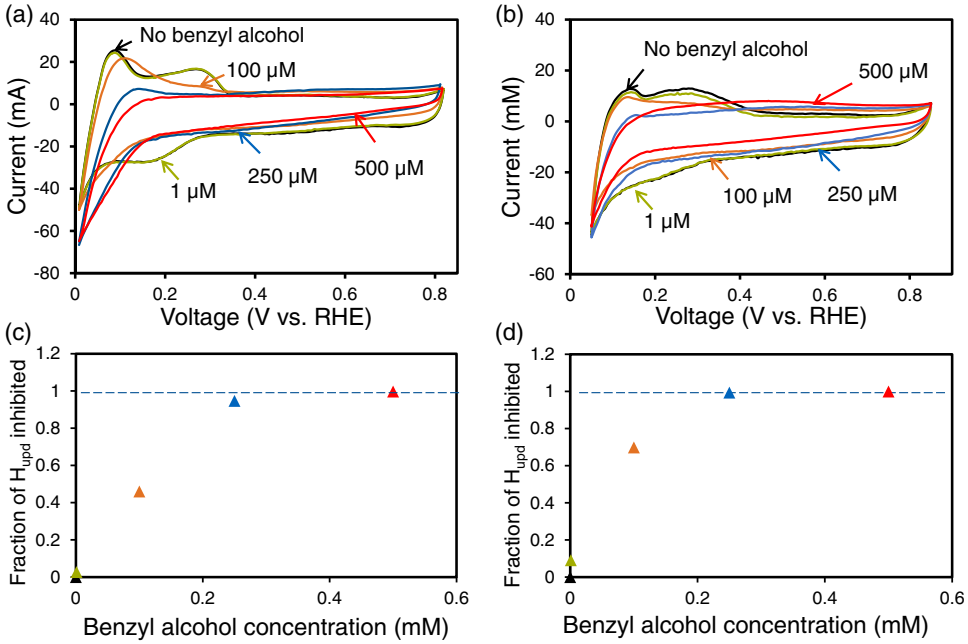

Fig. 2 | Influence of the benzyl alcohol concentration on the coverage of H on Pd/C. Cyclic voltammograms at a scan rate of 5 mV s^{-1} showing hydrogen underpotential deposition on Pd/C (30 wt.%) at room temperature with benzyl alcohol concentration varying from 0 to 500 μM and at **a** pH 2.5 in phosphate buffer solution and **b** pH 5 in acetate buffer solution. The calculated fraction of underpotentially deposited hydrogen that is inhibited on Pd vs. benzyl alcohol concentration **c** pH 2.5 in phosphate buffer solution and **d** pH 5 in acetate buffer solution, which is calculated from the decrease in H_{upd} charge relative to that without benzyl alcohol obtained from (**a**) and (**b**), respectively.

Possible reaction pathways

Three pathways to convert benzyl alcohol to toluene are conceivable, i.e., (i) direct hydrogenolysis (Fig. 4a), (ii) partial hydrogenation–dehydration–re-hydrogenation ((Fig. 4b),) and (iii) protonation–dehydration–hydride addition (Fig. 4c).

In the first pathway, benzyl alcohol adsorbs on Pd molecularly (BA_{ad}); dissociatively adsorbed H_2 acts as the reducing agent (H_{ad}). Then, following an SN_2 mechanism, H_{ad} attacks the benzylic carbon and displaces the hydroxyl group, leading to the formation of toluene[28]. This pathway has hydrogen involved in all relevant cleavage steps and is incompatible with the absence of an isotope effect.

In the second reaction pathway, benzyl alcohol and H_2 are adsorbed and the aromatic ring of benzyl alcohol is partial hydrogenated providing a β-H. The intramolecular dehydration yields the olefin product, followed by hydrogen addition leading to toluene and/or hydrogenation to 5-methylcyclohexa-1,3-diene. This mechanism is similar to that reported for C–O bond cleavage of 1-(4-isobutylphenyl) ethanol over Pd supported on acidic carbon[19]. As benzyl alcohol does not have a hydrogen in the β position for dehydration, the aromatic ring needs to be partly hydrogenated, in analogy to the reductive solvolysis of aryl ethers[3,33]. This reaction pathway is also excluded, because 5-methylcyclohexa-1,3-diene was not detected, and deuterium was not observed in the aromatic ring for reactions performed in D_2 and D_2O (SI, Note S1).

Thus, the third pathway, water elimination upon protonation of the hydroxyl group to a carbocation in presence of hydronium ions is concluded to be the most likely reaction pathway and will be further analyzed in detail.

Table 1 | Summary of reaction rates and reaction orders

pH	TOF (mol $mol_{Pd}^{-1}h^{-1}$)[a]	Reaction order benzyl alcohol (α)	Reaction order H_2 (β)
2.5	527	0.08	0.09
5	162	−0.01	0.09

[a]TOF at 1 bar H_2 and 298 K with a benzyl alcohol concentration of 20 mM.

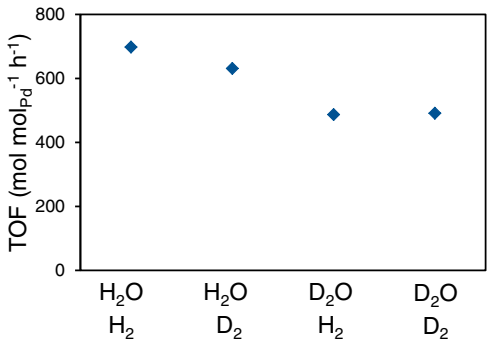

Fig. 3 | Turnover rates of benzyl alcohol hydrogenolysis in H_2O-H_2, H_2O-D_2, D_2O-H_2, and D_2O-D_2. Reaction condition: at 298 K and atmospheric pressure with a benzyl alcohol concentration of 20 mM on Pd/C and 0.2 M phosphoric acid.

Factors influencing benzyl alcohol hydrogenolysis

The elementary steps of the pathway are shown in Fig. 4c. It should be emphasized that the presence of water, H_2, and $H_3O^+_{(hydr.)}$ will lead to establishing the corresponding OCP at the surface, which enables quasi-equilibrated interconversion of the species involving electrons of Pd.

The electrochemical quasi-equilibrium (hydrogen electrode reaction) will be established between all species on the metal surface establishing the OCP, as shown in the reaction equation Rxn 2 (Step g in Fig. 4c).

$$H^* + H_2O \rightleftharpoons H_3O^+ + e^- + * \qquad \text{(Rxn2)}$$

The catalytic cycle starts with benzyl alcohol adsorption on vacant Pd sites (*) (Step a), afterwards, the adsorbed benzyl alcohol (BA*) is

https://doi.org/10.1038/s41467-022-35554-1

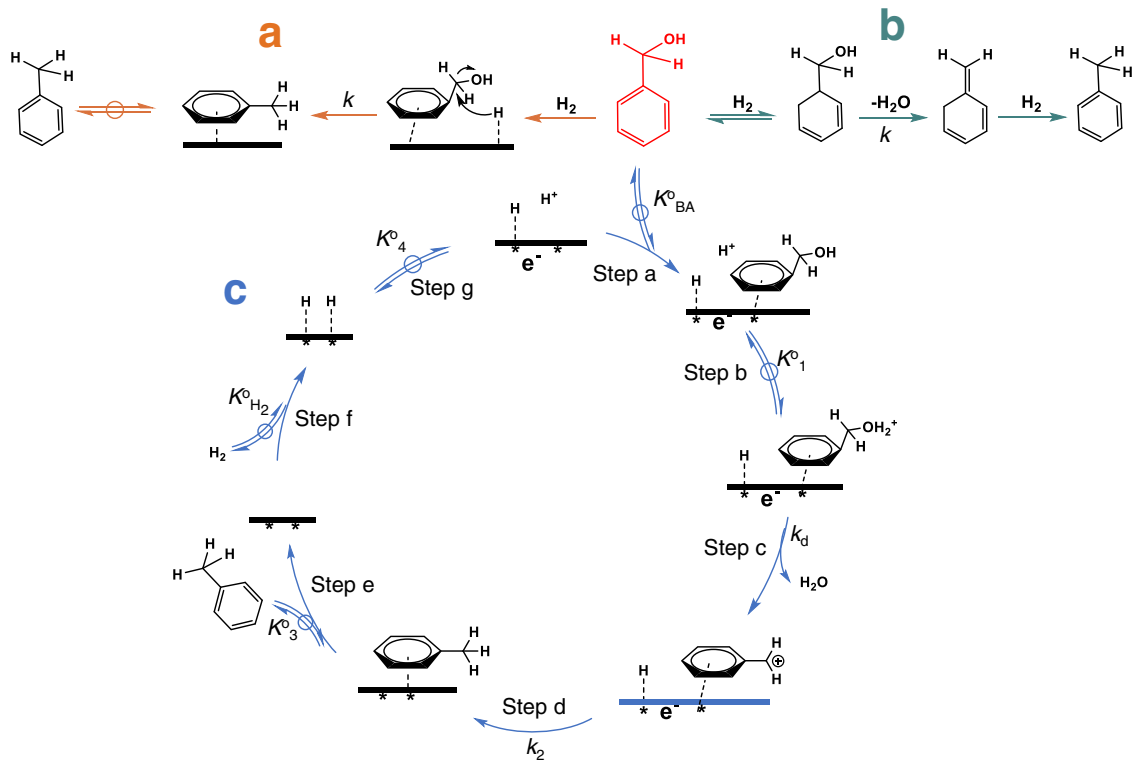

Fig. 4 | Reaction pathway of benzyl alcohol hydrogenolysis. a Direct hydrogenolysis, **b** partial hydrogenation– dehydration–re-hydrogenation and **c** protonation–dehydration–hydride addition (Fig. 4**c**). Elementary steps in Fig. 4**a**, **b** are omitted and the hydronium ion is expressed as proton in the scheme.

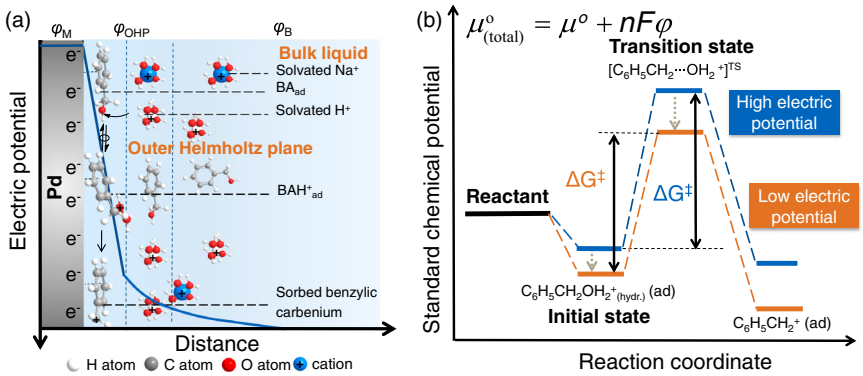

Fig. 5 | Schematic illustration of the rate-determining step and the energy diagram. a The Reaction steps of benzyl alcohol hydrogenolysis between Pd surface and Helmholtz plane and the potential profile as a function of distance from Pd surface. φ_M, φ_{OHP}, φ_B are potentials on Pd surface, at outer Helmholtz plane and in the bulk, respectively. **b** Standard chemical potential profiles of the initial state and transition state under low and high electric potentials.

protonated (Step b, $C_6H_5CH_2OH_2^{+*}$, BAH^{+*}), followed by elimination of water and the formation of the benzyl carbocation ($C_6H_5CH_2^{+*}$) (Step c). Toluene is then formed via hydride addition (Step d) and desorption from the Pd surface (Step e). H_2 dissociatively adsorbs on a Pd site pair (*-*), forming two adsorbed H atoms (H*) (Step f). The adsorption-desorption steps (Step a, e and f) are generally much faster and are, hence, considered to be quasi-equilibrated. Hydride addition (Step d) is not kinetic relevant, as a substantial KIE has not been observed when replacing H_2 by D_2. Therefore, the dehydration step (Step c) is considered to be rate-determining, when deriving the rate equation.

In aqueous phase, the OCP on the Pd surface induces an electrical double layer (EDL) at the Pd-water interface, where the Pd-catalyzed benzyl alcohol reduction occurs. Figure 5a shows the reaction elementary steps (Step b–c) in the space between the metal surface and outer Helmholtz plane (OHP). The chemisorbed species with their directed bonding to the surface, are located in the inner Helmholtz plane (IHP), while the nonspecifically adsorbed ions like hydrated hydronium ions and hydrated metal cations are located at the outer Helmholtz plane. The electric potential on Pd surface is determined by the equilibrium between H_2 and hydronium ion (Rxn 2). Under quasi-equilibrium conditions the OCP, i.e., the electrode potential of Pd, is expressed by the Nernst Equation (Eq. 2),

$$\varphi_M = \varphi_{SHE} + \frac{RT}{F}\ln\frac{a_{H^+}}{\sqrt{P_{H_2}}} \quad (2)$$

in which φ_{SHE} is standard hydrogen electrode potential (SHE) (defined as 0 V for convenience). The a_{H^+} is the hydronium ion activity in the bulk solution. It should be noted that φ_M is the electric potential

difference between Pd surface and electrolyte. The electric potential decays with distance from Pd surface until reaching the level of the bulk solution, which is considered as 0 V (Fig. 5a).

At the Pd surface, adsorbed H (H_{ad}), adsorbed benzyl alcohol (BA_{ad}), protonated benzyl alcohol (BAH^+_{ad}) and unoccupied sites (*) coexist. During a progressing reaction, a very small concentration of molecules in the transition state (TS) of the rate determining step must also exist (Fig. 4, step c). The expressions of chemical potentials or electrochemical potentials for all the species are

$$\mu_{BA_{aq}} = \mu^o_{BA_{aq}} + RT\ln a_{BA_{aq}} \tag{3}$$

$$\mu_{BA_{ad}} = \mu^o_{BA_{ad}} + RT\ln\frac{\theta_{BA_{ad}}}{\theta^*} \tag{4}$$

$$\mu_{H_2} = \mu^o_{H_2} + RT\ln P_{H_2} \tag{5}$$

$$\mu_{H_{ad}} = \mu^o_{H_{ad}} + RT\ln\frac{\theta_{H_{ad}}}{\theta^*} \tag{6}$$

$$\mu_{BAH^+_{ad}} = \mu^o_{BAH^+_{ad}} + RT\ln\frac{\theta_{BAH^+_{ad}}}{\theta^*} + F\varphi_{BAH^+_{ad}} \tag{7}$$

$$\mu_{H^+} = \mu^o_{H^+} + RT\ln a_{H^+} + F\varphi_B \tag{8}$$

$$\mu_{TS} = \mu^o_{TS} + RT\ln\frac{\theta_{TS}}{\theta^*} + F\varphi_{TS} \tag{9}$$

The μ_{BAaq}, μ_{BAad}, μ_{H_2}, μ_{Had}, μ_{H+}, μ_{BAH^+ad} and μ_{TS} are chemical or electrochemical potential of benzyl alcohol in bulk, sorbed benzyl alcohol, gas H_2, sorbed H, hydronium ion in bulk, sorbed protonated benzyl alcohol and transition state, respectively. The μ^o_{BAaq}, μ^o_{BAad}, $\mu^o_{H_2}$, μ^o_{Had}, μ^o_{H}+, $\mu^o_{BAH^+ad}$ and μ^o_{TS} are their corresponding chemical/electrochemical potential at standard state, defined at 1 bar H_2, 1 M concentration and a coverage of 0.5, respectively. The transition state (TS) and sorbed protonated benzyl alcohol (BAH^+_{ad}) are positively charged species, thus, they are considered to be located closer to the outer Helmholtz plane (Fig. 5a). The φ_{BAH^+ad}, φ_B and φ_{TS} are the electric potentials at the position of BAH^+_{ad}, bulk solution and transition state, respectively. Generally, φ_B is denoted as 0 V. It should be noted that the electrochemical potentials of the charged species BAH^+_{ad}, $H_3O^+_{(hydr.)}$ and TS are affected not only by the activity, but also by the electric potential at their located position. Figure 5b illustrates, how the electric potentials affect the chemical potential (free energy) of the charged reacting species. A more negative (low) electric potential stabilizes the cationic species, i.e., the initial state (benzyl alcohol oxonium ion), its dehydration transition state and the product (benzylic carbenium). The extent of stabilization depends on the location of these species in the EDL. Considering the hydrogen bonding at the outer Helmholtz layer, the transition state at a closer location to the Pd surface leads to a higher stabilization as it has less hydrogen bonding with water compared to the initial state, that consequently decreases their energy differences and the intrinsic energy barrier.

Because the dehydration step (Step c) is considered to be the RDS, the adsorption of substrate (Step a) and H_2 (Step f) as well as the protonation of benzyl alcohol (Step b) are considered to be quasi-equilibrated. This leads to several relations of chemical potentials,

$$\mu_{BA_{aq}} = \mu_{BA_{ad}} \tag{10}$$

$$\mu_{H_2} = 2\mu_{H_{ad}} \tag{11}$$

$$\mu_{BA_{ad}} + \mu_{H^+} = \mu_{BAH^+_{ad}} = \mu_{TS} \tag{12}$$

With these equations, the reaction rate is derived on basis of transition state theory as (derivation details in SI):

$$r = \frac{k_B T}{h}\frac{\exp\left(\frac{\mu_{BA_{aq}}+\mu_{H^+}-\mu^o_{TS}-F\varphi_{TS}}{RT}\right)}{1+\exp\left(\frac{1/2\mu_{H_2}-\mu^o_{H_{ad}}}{RT}\right)+\exp\left(\frac{\mu_{BA_{aq}}-\mu^o_{BA_{ad}}}{RT}\right)+\exp\left(\frac{\mu_{BA_{aq}}+\mu_{H^+}-\mu^o_{BAH^+_{ad}}-F\varphi_{BAH^+_{ad}}}{RT}\right)} \tag{13}$$

Thus, the reaction rate (Eq. 13) is affected by the chemical potentials of aqueous benzyl alcohol (μ_{BAaq}), hydronium ion (μ_{H+}) and H_2 (μ_{H_2}) as well as by φ_{TS} and φ_{BAH^+ad}. The chemical potentials are dependent on the benzyl alcohol concentration, $H_3O^+_{(hydr.)}$ concentration and H_2 pressure, respectively. To gauge the influence of each parameter influences the reaction, we introduce the partial derivative of the reaction rate to this parameter.

$$\frac{\partial lnr}{\partial \ln a_{BA_{aq}}} = RT\frac{\partial lnr}{\partial \mu_{BA_{aq}}} = 1 - \theta_{BA_{ad}} - \theta_{BAH^+_{ad}} \tag{14}$$

$$\frac{\partial lnr}{\partial \ln P_{H_2}} = -\frac{1}{2}\theta_{H_{ad}} + \frac{\partial\varphi_{TS}}{2\partial\varphi_M} - \theta_{BAH^+_{ad}}\frac{\partial\varphi_{BAH^+_{ad}}}{2\partial\varphi_M} \tag{15}$$

$$\frac{\partial lnr}{\partial \ln a_{H^+}} = 1 - \theta_{BAH^+_{ad}} - \frac{\partial\varphi_{TS}}{\partial\varphi_M} + \theta_{BAH^+_{ad}}\frac{\partial\varphi_{BAH^+_{ad}}}{\partial\varphi_M} \tag{16}$$

$$\frac{\partial lnr}{\partial\varphi_M} = \frac{F}{RT}\left(-\frac{\partial\varphi_{TS}}{\partial\varphi_M} + \theta_{BAH^+_{ad}}\frac{\partial\varphi_{BAH^+_{ad}}}{\partial\varphi_M}\right) \tag{17}$$

Equations 14, 15 and 16 represent the reaction orders with respect to benzyl alcohol, H_2 and $H_3O^+_{(hydr.)}$. It is noticeable that their reaction orders are functions of the coverages of corresponding species. In particular, the reaction orders of H_2 and $H_3O^+_{(hydr.)}$ contain the term φ_M (Eqs. 15 and 16), indicating that they can influence the reaction rate by changing the electric potential on Pd because they are involved in the hydrogen electrode reaction, establishing the OCP. On the other hand, benzyl alcohol does not affect the electric potential, so its reaction order expression does not contain φ_M (Eq. 14). The measured reaction order of benzyl alcohol was 0, indicating the $(\theta_{BA} + \theta_{BAH^+_{ad}})$ being 1 according to Eq. 14, and meaning Pd surface is fully saturated by benzyl alcohol and its protonated form BAH^+. This agrees perfectly with the CV measurements (Fig. 2) that Pd surface is saturated with benzyl alcohol and derived species.

The influence of electric potential φ_M on the rate is expressed in Eq. 17. To verify this, Pd/C was loaded on an electrode and exposed to a negative electric potential (vs. SHE). Figure 6 shows the conversion rate of benzyl alcohol to toluene at pH 1.6 under different electric potentials. A larger reaction rate was observed under a more negative electric potential. Stabilizing the carbenium ion product after dehydration, is concluded to lead to a lower transition state following the Polanyi relation[34]. We assume that transition state is closer to Pd surface compared to protonated benzyl alcohol (BAH^+), as it will be then less hydrogen bonded in the aqueous environment.

It is unclear whether H_2 competes for the active sites on Pd or whether it adsorbs in between adsorbed benzyl alcohol molecules[31]. Under the conditions studied this effect is negligible due to the small coverage of H_{ad}. Therefore, we conclude that the main effect of H_2 on the reaction rate is related to its influence via φ_M (Eq. 15). A higher H_2 pressure is equivalent to a more negative φ_M (Eq. 2).

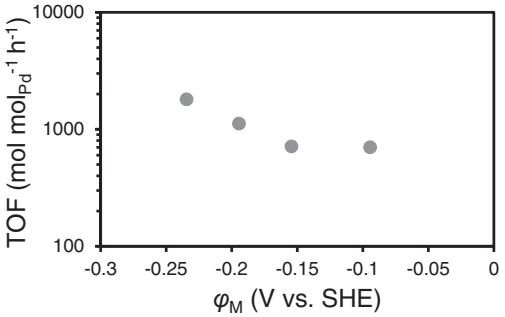

Fig. 6 | TOF as a function of electric potential of Pd at pH 1.6. Reaction condition: 10 mg Pd/C (5wt.%) at 298 K.

The $H_3O^+_{(hydr.)}$ concentration is directly related to the concentration of BAH^+_{ad}, and the reaction order in $H_3O^+_{(hydr.)}$ can partially reflect the relative abundance of BA_{ad} and BAH^+_{ad} on Pd surface (the none electric potential related part in Eq. 16). This agrees with the changing reaction order in $H_3O^+_{(hydr.)}$ during the whole pH range from pH 0.6 to pH 7 (Fig. 1b) and the fact that a smaller reaction order was obtained at a lower pH. However, increasing $H_3O^+_{(hydr.)}$ concentration also increases φ_M, which inhibits the reaction. As shown in Fig. 7, for each pH, the reaction rate increases with H_2 pressure, caused by the decreasing of electric potential at either OCP or under external electric potentials. In comparison, to decrease pH can be resolved into two components: BAH^+_{ad} coverage (or transition state concentration) increasing and φ_M increasing. Apparently, the increase in BAH^+_{ad} coverage overcomes the negative influence by the increase of the electric potential, and leads to the increased reaction rate with decreasing pH.

It is shown that the reductive elimination of benzyl alcohol catalyzed by Pd/C is highly sensitive to the quasi-equilibrated electrochemical steps at the metal-water interface. The conversion rate of benzyl alcohol hydrogenolysis increased by 2–3 orders of magnitude with decreasing the pH from 7 to 0.6. Kinetic analysis and isotope-labeling study show that the reaction follows a pathway of protonating benzyl alcohol at the hydroxyl group, followed by elimination of water to form a benzyl carbenium ion, and hydride addition to the benzyl carbenium ion to form toluene. The elimination to form the benzyl carbenium ion is concluded to determine the overall reaction rate.

Acting as proton donor, a high $H_3O^+_{(hydr.)}$ activity increases the reaction rate by increasing the concentration of the reacting initial state (BAH^+_{ad}) due to the higher probability of protonation. Besides this conventional effect, $H_3O^+_{(hydr.)}$ also influences the OCP. The OCP is the electric potential established by the quasi-equilibrated electrode reaction of H_2 and $H_3O^+_{(hydr.)}$ at the metal-water interface; it decreases with H_2 pressure (negative correlation) and increases with the activity of $H_3O^+_{(hydr.)}$ (positive correlation). As positively charged species, both the reacting initial state (BAH^+_{ad}) and its dehydration transition state are stabilized by the negative electric potential at the metal-water interface. Because of the strong hydrogen bonding at the outer Helmholtz layer, the benzyl carbenium ion intermediate is closer to the metal surface, as it has less hydrogen bonding with water compared to the initial state (BAH^+_{ad}). Thus, the negative charge at the metal surface provides relative more stabilization to the benzyl carbenium ion, that consequently decreases their energy differences and the reaction energy barrier. Such effect is weakened at higher activities of $H_3O^+_{(hydr.)}$ because of the less negative OCP.

By influencing OCP, H_2 also influences the conversion rate, although H_2 as a reactant is only involved in the steps after rate determining step. A high pressure of H_2 corresponds to a more negative OCP, resulting in a lower activation energy and higher reaction rate. The results highlight the complex interplay that needs to be considered, when interpreting reactions at the water-metal interface. More general, it underlines the importance of OCP at the solid-aqueous interface for the reactions involving charged reactants, intermediates and transition states.

Methods

Chemicals and catalyst

Pd/C catalyst with a Pd content of 5 wt.% was purchased from Sigma Aldrich. The Pd particle size is 2.9 nm on average measured by TEM, and metal dispersion is 33% measured by H_2 adsorption. All chemicals were obtained from commercial suppliers and used as received, including benzyl alcohol (Sigma-Aldrich, ≥99.0%) and chemicals for buffer solutions (Sigma-Aldrich, ≥99.9%, e.g., $HClO_4$, H_3PO_4, NaH_2PO_4, Na_2HPO_4, H_2SO_4, Na_2SO_4, CH_3COOH, CH_3COONa), NaCl (Sigma-Aldrich, ≥99.9%), ethyl acetate (Sigma-Aldrich, ≥99.9%, HPLC), and 2-cyclohexen-1-one (Sigma Aldrich, >99%). High purity water, treated with a Milli-Q water purification system until a resistivity of 18.2 MΩ cm, was used in all experiments. H_2 (Air Liquide, >99.99%) was used for hydrogenation.

Catalyst characterization

The specific surface area of the catalyst was determined (according to BET) from N_2 physisorption, which were measured at 77 K on a PMI automated BET sorptometer. The samples were first outgassed at 523 K in vacuum (<0.001 mbar) for 20 h before measurement.

The dispersion of the metals was determined by H_2 chemisorption on Thermo Scientific Surfer Analyzer. The Pd/C catalysts were treated in vacuum at 588 K for 1 h and then cooled to 313 K. A first set of H_2 adsorption isotherm was measured from 1 to 40 kPa. Afterwards, the samples were outgassed at the same temperature for 1 h to remove the physisorbed H_2, followed by a second set of isotherms being measured, which corresponded to physisorbed H_2. The difference of the two isotherms was the chemisorbed hydrogen on Pd. The concentrations of surface Pd atoms were determined by extrapolating the saturated region of the difference isotherms to zero hydrogen pressure and using the value as the number of surface Pd atoms assuming a stoichiometry of one hydrogen to one Pd atom. Then the dispersion of Pd was calculated by comparing the surface Pd atoms to the total Pd atoms.

The size of Pd particle was determined by transmission electron microscopy (TEM, JEOL JEM-2011) with an accelerating voltage of 120 keV. Statistical treatment of the metal particle size was done by counting at least 300 particles detected in several places of the grid. The Pd/C used in this work is the same as in our previous work and the TEM image[4].

Catalytic reaction measurements under OCP (open circuit potential)

Benzyl alcohol hydrogenolysis was carried out in a batch reactor with 5–10 mg Pd/C (5 wt.% Pd loading) in 0.2 M buffer solution. Typical measurements under atmospheric pressure were performed with H_2 or diluted H_2 using N_2 (flow rate of 10 mL min^{-1}) flowing through the reactant solution at 296 K and 600 rpm. Reactions at higher H_2 pressures were performed in a 300 mL Hastelloy PARR reactor, and air was removed from the reactor by introducing 20 bar H_2, followed by depressurizing the reactor for three times. The benzyl alcohol concentration was 20 mM. After the reaction, the solution was extracted using ethyl acetate with 2-cyclohexen-1-one as the internal standard for quantification. NaCl was used to increase the extraction efficiency. The extracted ethyl acetate was treated with Na_2SO_4 to remove dissolved water. Quantitative analyses of the samples were performed by gas chromatography equipped with a Wax capillary column (30 m × 250 μm) and a flame ionization detector (FID). Reaction orders of H_2 were determined by changing H_2 pressure from 0.2 bar to 20 bar.

The reactions in D_2O or/and D_2 were carried out in a 100 mL Hastelloy PARR reactor. 20 mM benzyl alcohol, 30 mL 0.2 M D_3PO_4

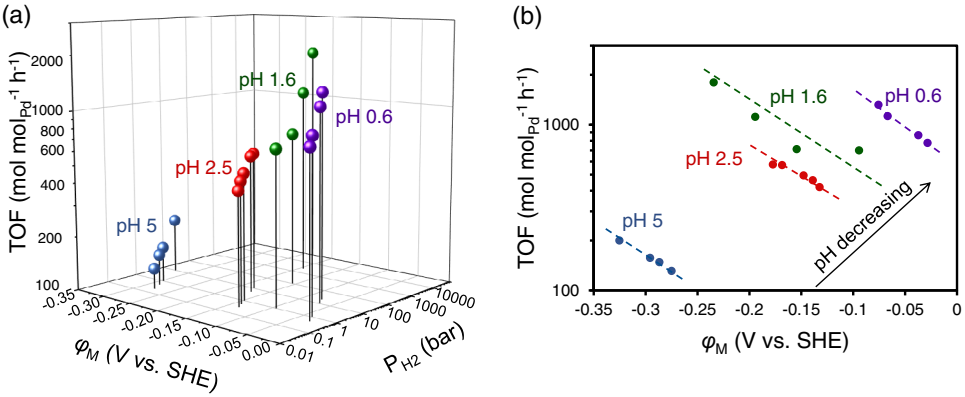

Fig. 7 | Comparison of the reaction rates at OCV and external electric potentials. a TOF as a function of electric potential of Pd (φ_M) and P_{H_2} at OCP under pH 0.6 (0.5–20 bar), pH 2.5 (0.3–10 bar) and pH 5 (0.2–10 bar) and external electric potential at pH 1.6 on Pd/C (5wt.%) at 298 K. **b** The corresponding projection onto the plane of TOF vs. φ_M. A hypothetical P_{H_2} is used for pH 1.6 that is equilibrated with the externally added electric potentials.

solution in D_2O (99.8%, Sigma), 1 bar D_2 and 10 mg Pd/C were sealed in the reactor for reaction at 296 K and 750 rmp. Before the reaction, air was removed from the reactor by introducing 20 bar D_2, followed by depressurizing the reactor for three times. After the experiment, ethyl acetate was used to extract the chemical species and then were quantified using GC-MS equipped with a HP-5 capillary column.

Electrocatalytic reaction

Experiments were carried out in a H cell with a Nafion 117 proton exchange membrane (Ion Power, Inc.) to separate the cathodic and anodic compartments. An electrochemical workstation VSP-300, Bio Logic was used to perform electrochemical procedures. A piece of carbon felt (Alfa Aesar >99.0%, 3.2 mm thickness) infiltrated with 10 mg Pd/C connected to a graphite rod (Sigma Aldrich, 99.99%) was used as working electrode in the cathode compartment. A platinum wire (Alfa Aesar, 99.9%) was used as counter electrode in the anodic compartment. Ag/AgCl was used as a reference electrode. The cathode and anode compartments were filled with 60 mL 0.2 M H_3PO_4 solution as electrolyte solution. All reactions were performed at atmospheric pressure at constant potential referred to the reverse hydrogen electrode (RHE). The catalyst was first activated under a constant current of −40 mA for 10 min before adding benzyl alcohol (20 mM) into the cathode compartment. Then an electric potential was applied for reaction. Product analysis is the same as performed in the catalytic reaction under OCP.

Cyclic voltammetry

The coverage of benzyl alcohol on Pd surface was determined via cyclic voltammetry in a Teflon H-cell with a Nafion 117 proton exchange membrance to separate cathodic and anodic compartments. 20 mg Pd/C (30 wt%, Sigma Aldrich) on carbon felt (Alfa Aesar >99.0%, 3.2 mm thickness) was used as working electrode, a Ag/AgCl electrode with double-junction was used as reference electrode, and a platinum wire (Alfa Aesar, 99.9 %) was used as counter electrode. The electrolytes are phosphate buffer (pH 2.5) and acetate buffer (pH 5). The cyclic voltammetry was measured at 5 mV s^{-1} with 20 mL min^{-1} N_2 bubbling, and under different concentrations of benzyl alcohol. The sites blocked by benzyl alcohol (benzyl alcohol coverage) was calculated based on the area difference of the underpotentially deposited hydrogen (H_{upd}) peak before and after the benzyl alcohol addition[35]. The same measurement was also performed on Pd/C (5 wt.%), but it was difficult to distinguish the H_{upd} peak from the double layer capacitance background current induced by the carbon support.

Data availability

All data are available within the paper and its Supplementary Information files and Source Data file. Source data are provided with this paper.

References

1. Gallezot, P. Conversion of biomass to selected chemical products. *Chem. Soc. Rev.* **41**, 1538–1558 (2012).
2. Corma, A., Iborra, S. & Velty, A. Chemical routes for the transformation of biomass into chemicals. *Chem. Rev.* **107**, 2411–2502 (2007).
3. Wang, M., Shi, H., Camaioni, D. M. & Lercher, J. A. Palladium-catalyzed hydrolytic cleavage of aromatic C–O bonds. *Angew. Chem. Int. Ed.* **56**, 2110–2114 (2017).
4. Cheng, G. et al. Critical role of solvent-modulated hydrogen-binding strength in the catalytic hydrogenation of benzaldehyde on palladium. *Nat. Catal.* **4**, 976–985 (2021).
5. Mellmer, M. A. et al. Solvent-enabled control of reactivity for liquid-phase reactions of biomass-derived compounds. *Nat. Catal.* **1**, 199–207 (2018).
6. Varghese, J. J. & Mushrif, S. H. Origins of complex solvent effects on chemical reactivity and computational tools to investigate them: a review. *React. Chem. Eng.* **4**, 165–206 (2019).
7. Takenouchi, M., Kudoh, S., Miyajima, K. & Mafuné, F. Adsorption and desorption of hydrogen by gas-phase palladium clusters revealed by in situ thermal desorption spectroscopy. *J. Phys. Chem. A* **119**, 6766–6772 (2015).
8. Pang, S. H., Román, A. M. & Medlin, J. W. Adsorption orientation-induced selectivity control of reactions of benzyl alcohol on Pd(111). *J. Phys. Chem. C* **116**, 13654–13660 (2012).
9. Hensley, A. J. R., Bray, J., Shangguan, J., Chin, Y.-H. & McEwen, J.-S. Catalytic consequences of hydrogen addition events and solvent-adsorbate interactions during guaiacol-H2 reactions at the H2O-Ru(0 0 0 1) interface. *J. Catal.* **395**, 467–482 (2021).
10. Shangguan, J. et al. The role of protons and hydrides in the catalytic hydrogenolysis of guaiacol at the ruthenium nanoparticle–water interface. *ACS Catal.* **10**, 12310–12332 (2020).
11. Akpa, B. S. et al. Solvent effects in the hydrogenation of 2-butanone. *J. Catal.* **289**, 30–41 (2012).
12. Strmcnik, D. et al. The role of non-covalent interactions in electrocatalytic fuel-cell reactions on platinum. *Nat. Chem.* **1**, 466–472 (2009).
13. Zhao, Z. et al. Solvent-mediated charge separation drives alternative hydrogenation path of furanics in liquid water. *Nat. Catal.* **2**, 431–436 (2019).

14. Sanyal, U. et al. Hydrogen bonding enhances the electrochemical hydrogenation of benzaldehyde in the aqueous phase. *Angew. Chem. Int. Ed.* **60**, 290–296 (2021).
15. Akhade, S. A. et al. Electrocatalytic hydrogenation of biomass-derived organics: a review. *Chem. Rev.* **120**, 11370–11419 (2020).
16. Singh, N. et al. Impact of pH on aqueous-phase phenol hydrogenation catalyzed by carbon-supported Pt and Rh. *ACS Catal.* **9**, 1120–1128 (2019).
17. Ryu, J. & Surendranath, Y. Tracking electrical fields at the Pt/H2O interface during hydrogen catalysis. *J. Am. Chem. Soc.* **141**, 15524–15531 (2019).
18. Ryu, J., Wuttig, A. & Surendranath, Y. Quantification of interfacial pH variation at molecular length scales using a concurrent non-Faradaic reaction. *Angew. Chem. Int. Ed.* **57**, 9300–9304 (2018).
19. Thakar, N. et al. Deuteration study to elucidate hydrogenolysis of benzylic alcohols over supported palladium catalysts. *J. Catal.* **246**, 344–350 (2007).
20. Liu, X. et al. Catalytic transfer hydrogenolysis of 2-phenyl-2-propanol over palladium supported on activated carbon. *J. Mol. Catal. A: Chem.* **252**, 176–180 (2006).
21. Sawadjoon, S., Lundstedt, A. & Samec, J. S. M. Pd-catalyzed transfer hydrogenolysis of primary, secondary, and tertiary benzylic alcohols by formic acid: a mechanistic study. *ACS Catal.* **3**, 635–642 (2013).
22. Ranade, V. S. & Prins, R. Hydrogenolysis of benzylic alcohols on rhodium catalysts. *Chem. Eur. J.* **6**, 313–320 (2000).
23. Nakagawa, Y., Tamura, M. & Tomishige, K. Catalytic materials for the hydrogenolysis of glycerol to 1,3-propanediol. *J. Mater. Chem.* **2**, 6688–6702 (2014).
24. Zhu, S. et al. Alkaline metals modified Pt–H4SiW12O40/ZrO2 catalysts for the selective hydrogenolysis of glycerol to 1,3-propanediol. *Appl. Catal. B: Environ.* **140-141**, 60–67 (2013).
25. Malyala, R. V., Rode, C. V., Arai, M., Hegde, S. G. & Chaudhari, R. V. Activity, selectivity and stability of Ni and bimetallic Ni–Pt supported on zeolite Y catalysts for hydrogenation of acetophenone and its substituted derivatives. *Appl. Catal. A: Gen.* **193**, 71–86 (2000).
26. Kwak, B.-S., Kim, T.-J. & Lee, S.-I. Hydrogenolysis of α-methylbenzyl alcohol over bifunctional catalysts. *Appl. Catal. A: Gen.* **238**, 141–148 (2003).
27. Lin, H.-W., Yen, C. H. & Tan, C.-S. Aromatic hydrogenation of benzyl alcohol and its derivatives using compressed CO2/water as the solvent. *Green. Chem.* **14**, 682–687 (2012).
28. Kieboom, A. P. G., De Kreuk, J. F. & Van Bekkum, H. Substituent effects in the hydrogenolysis of benzyl alcohol derivatives over palladium. *J. Catal.* **20**, 58–66 (1971).
29. Ley, S. V., Stewart-Liddon, A. J., Pears, D., Perni, R. H. & Treacher, K. Hydrogenation of aromatic ketones, aldehydes, and epoxides with hydrogen and Pd(0)EnCat 30NP. *Beilstein J. Org. Chem.* **2**, 15 (2006).
30. Singh, N. et al. Carbon-supported Pt during aqueous phenol hydrogenation with and without applied electrical potential: X-ray absorption and theoretical studies of structure and adsorbates. *J. Catal.* **368**, 8–19 (2018).
31. Koh, K. et al. Electrochemically tunable proton-coupled electron transfer in Pd-catalyzed benzaldehyde hydrogenation. *Angew. Chem. Int. Ed.* **59**, 1501–1505 (2020).
32. Song, Y. et al. Hydrogenation of benzaldehyde via electrocatalysis and thermal catalysis on carbon-supported metals. *J. Catal.* **359**, 68–75 (2018).
33. Wang, M., Gutiérrez, O. Y., Camaioni, D. M. & Lercher, J. A. Palladium-catalyzed reductive insertion of alcohols into aryl ether bonds. *Angew. Chem. Int. Ed.* **57**, 3747–3751 (2018).
34. Shetty, M. et al. Directing the rate-enhancement for hydronium ion catalyzed dehydration via organization of alkanols in nanoscopic confinements. *Angew. Chem. Int. Ed.* **60**, 2304–2311 (2021).
35. Connolly, J. F., Flannery, R. J. & Aronowitz, G. Electrochemical measurement of the available surface area of carbon-supported platinum. *J. Electrochem. Soc.* **113**, 577 (1966).

Acknowledgements

G.C. is grateful to the Chinese Scholarship Council for the financial support. J.A.L. and O.Y.G. acknowledge the support by the U.S. Department of Energy (DOE), Office of Science, Office of Basic Energy Sciences (BES), Division of Chemical Sciences, Geosciences and Biosciences (Impact of catalytically active centers and their environment on rates and thermodynamic states along reaction paths, FWP 47319). Y.L. and W.Z. acknowledge the support by the Open Project Program of Academician and Expert Workstation, Shanghai Curui Low-Carbon Energy Technology Co., Ltd.

Author contributions

G.C. carried out the reactions and performed the characterizations of catalysts. W.Z., A.J., E.E.E., and O.Y.G. cooperated with the discussion and provided valuable suggestions. Y.L. and J.A.L. supervised the work and provided guidance throughout the project. The manuscript was written through contributions of all authors. All authors have given approval to the final version of the manuscript.

Funding

Open Access funding enabled and organized by Projekt DEAL.

Competing interests

The authors declare no competing interests.

Additional information

Supplementary information The online version contains supplementary material available at https://doi.org/10.1038/s41467-022-35554-1.

Correspondence and requests for materials should be addressed to Yue Liu or Johannes A. Lercher.

Peer review information *Nature Communications* thanks Bin Wang and the other, anonymous, reviewer for their contribution to the peer review of this work. Peer reviewer reports are available.